The Role of Histogram-Based Textural Analysis of ^{18}F-FDG PET/CT in Evaluating Tumor Heterogeneity and Predicting the Prognosis of Invasive Lung Adenocarcinoma

İnvaziv Akciğer Adenokarsinomunda ^{18}F-FDG PET/CT Histograma Dayalı Doku Analizinin Tümör Heterojenitesinin Değerlendirilmesinde ve Prognoz Tayininde Rolü

⑩ *Hasan Önner[1]*, ⑩ *Nazım Coşkun[2]*, ⑩ *Mustafa Erol[1]*, ⑩ *Meryem İlkay Eren Karanis[3]*

[1]University of Health Sciences Turkey, Konya City Hospital, Clinic of Nuclear Medicine, Konya, Turkey
[2]University of Health Sciences Turkey, Ankara City Hospital, Clinic of Nuclear Medicine, Ankara, Turkey
[3]University of Health Sciences Turkey, Konya City Hospital, Clinic of Pathology, Konya, Turkey

Abstract

Objectives: This study aimed to investigate the contributory role of histogram-based textural features (HBTFs) extracted from ^{18}fluorine-fluorodeoxyglucose (^{18}F-FDG) positron emission tomography/computed tomography (PET/CT) in tumoral heterogeneity (TH) evaluation and invasive lung adenocarcinoma (ILA) prognosis prediction.

Methods: This retrospective study analyzed the data of 72 patients with ILA who underwent ^{18}F-FDG PET/CT followed by surgical resection. The maximum standardized uptake value (SUV$_{max}$), metabolic tumor volume, and total lesion glycolysis values were calculated for each tumor. Additionally, HBTFs were extracted from ^{18}F-FDG PET/CT images using the software program. ILA was classified into the following five histopathological subtypes according to the predominant pattern: Lepidic adenocarcinoma (LA), acinar adenocarcinoma, papillary adenocarcinoma, solid adenocarcinoma (SA), and micropapillary adenocarcinoma (MA). Differences between ^{18}F-FDG PET/CT parameters and histopathological subtypes were evaluated using non-parametric tests. The study endpoints include overall survival (OS) and progression-free survival (PFS). The prognostic values of clinicopathological factors and ^{18}F-FDG PET/CT parameters were evaluated using the Cox regression analyses.

Results: The median SUV$_{max}$ and entropy values were significantly higher in SA-MA, whereas lower in LA. The median energy-uniformity value of the LA was significantly higher than the others. Among all parameters, only skewness and kurtosis were significantly associated with lymph node involvement status. The median values for follow-up time, PFS, and OS were 31.26, 16.07, and 20.87 months, respectively. The univariate Cox regression analysis showed that lymph node involvement was the only significant predictor for PFS. The multivariate Cox regression analysis revealed that higher SUV$_{max}$ (≥11.69) and advanced stage (IIB-IIIA) were significantly associated with poorer OS [hazard ratio (HR): 3.580, p=0.024 and HR: 7.608, p=0.007, respectively].

Conclusion: HBTFs were tightly associated with clinicopathological factors causing TH. Among the ^{18}F-FDG PET/CT parameters, only skewness and kurtosis were associated with lymph node involvement, whereas SUV$_{max}$ was the only independent predictor of OS. TH measurement with HBTFs may contribute to conventional metabolic parameters in guiding precision medicine for ILA.

Keywords: Lung adenocarcinoma, prognosis, fluorodeoxyglucose, textural analysis, radiomics

Öz

Amaç: Bu çalışmada, invaziv akciğer adenokarsinomunda (IAA) ^{18}flor-florodeoksiglukoz (^{18}F-FDG) pozitron emisyon tomografisi/bilgisayarlı tomografiden (PET/BT) elde edilen histogram tabanlı doku özelliklerinin (HTDÖ) tümör heterojenitesini (TH) ve prognozu değerlendirmedeki katkı rolü araştırılmıştır.

Yöntem: Cerrahi tedavi öncesi ^{18}F-FDG PET/BT tetkiki uygulanan ve primer tümörü rezeke edilen 72 IAA'lı hastanın verileri geriye dönük olarak incelendi. Her primer tümör için maksimum standardize alım değeri (SUV$_{maks}$), metabolik tümör hacmi ve toplam lezyon glikoliz değerleri hesaplandı. Ayrıca yazılım programı kullanılarak HTDÖ'ler edildi. IAA, baskın histopatolojik alttipe göre beş gruba ayrıldı: Lepidik adenokarsinom (LA), asiner adenokarsinom, papiller adenokarsinom, solid adenokarsinom (SA) ve mikropapiller adenokarsinom (MA). ^{18}F-FDG PET/BT parametreleri ve histopatolojik alt tipler arasındaki farklılıklar non-parametrik testler ile değerlendirildi. Çalışma sonlanım noktaları genel sağkalım (SK) ve progresyonsuz sağkalım (PSK) idi. Klinikopatolojik faktörlerin ve ^{18}F-FDG PET/BT parametrelerinin prognostik değerleri Cox regresyon analizi ile değerlendirildi.

Bulgular: Medyan SUV$_{maks}$ ve medyan entropy değerleri SA-MA'da anlamlı olarak yüksek, LA'da daha düşük olarak bulundu. LA'nın medyan energy-uniformity değeri diğerlerinden anlamlı derecede yüksekti. Tüm parametreler arasında sadece skewness ve kurtosis, lenf nodu tutulumu durumu ile anlamlı olarak ilişkiliydi. Takip süresi, PSK ve SK için medyan değerler sırasıyla; 31,26, 16,07 ve 20,87 aydı. Tek değişkenli Cox regresyon analizi, lenf nodu tutulumunun PSK için tek anlamlı öngörücü olduğunu gösterdi. Çok değişkenli Cox regresyon analizi, yüksek SUV$_{maks}$ (≥11,69) ve ileri evrenin (IIB-IIIA) daha kötü SK ile anlamlı şekilde ilişkili olduğunu ortaya koydu [sırasıyla; hazard ratio (HR): 3,580, p=0,024 ve HR: 7,608, p=0,007].

Sonuç: HDTÖ'ler, TH'ye neden olan klinikopatolojik faktörlerle yakından ilişkiydi. ^{18}F-FDG PET/BT parametrelerinden sadece skewness ve kurtosis lenf nodu tutulumu ile ilişkiliydi. SUV$_{maks}$, OS'nin bağımsız öngörücüsü olan tek ^{18}F-FDG PET/BT parametresiydi. TH'nin HBTF'lerle ölçümü, ILA için hassas tıbbın yönlendirilmesinde geleneksel metabolik parametrelere katkıda bulunabilir.

Anahtar kelimeler: Akciğer adenokarsinomu, prognoz, florodeoksiglukoz, doku analizi, radyomiks

Introduction

Lung cancer is the leading cause of cancer deaths worldwide (1). Surgical resection is a radical treatment for early-stage non-small cell lung cancer (NSCLC); however, ~40-60% of patients with early-stage NSCLC die within 5 years following curative resection. Approximately 85% of lung cancer consists of invasive lung adenocarcinoma (ILA), which is the most common histopathological subtype among NSCLC and has a poor prognosis (2). ILA consist of mixed patterns and exhibit highly heterogeneous behavior. The current histopathological classification of ILA fails to meet the advances in imaging, pathology, and tumor molecular biology (3). Additionally, this classification was inefficient for precision medicine development and prognosis prediction. Therefore, in the new classification, ILA is divided into the following five histopathological subtypes based on the dominant pattern: Lepidic adenocarcinoma (LA), acinar adenocarcinoma (AA), papillary adenocarcinoma (PA), solid adenocarcinoma (SA), and micropapillary adenocarcinoma (MA) (3).

Tumor heterogeneity (TH) is one of the important factors that affect treatment response (4). TH, as assessed by [18]fluorine-fluorodeoxyglucose (^{18}F-FDG) positron emission tomography/computed tomography (PET/CT), reflects intra-tumoral variabilities, such as cellularity, proliferation, and necrosis (5). Texture analysis is a set of quantitative parameters that reflect TH using computational processing techniques (6). This analysis shows that heterogeneity is quantitated in all tumor areas in ^{18}F-FDG uptake. With textural analysis, lots of studies have been conducted in various areas, such as benign-malignant distinction (7,8), tumor subtype differentiation (9), treatment response evaluation (10,11), and prognosis prediction (12,13).

Several studies have evaluated the association of histopathological patterns of ILA with conventional ^{18}F-FDG PET/CT parameters, such as maximum standardized uptake value (SUV$_{max}$), metabolic tumor volume (MTV), and total lesion glycolysis (TLG) (14,15,16). However, studies that investigated the relationship between histopathological patterns of resected ILA and histogram-based textural features (HBTFs) extracted from ^{18}F-FDG PET/CT are scarce.

Therefore, this study evaluated ^{18}F-FDG PET/CT parameters along with HBTFs to evaluate TH and identify independent predictors of progression-free survival (PFS) and overall survival (OS) of ILA. In light of our findings, different postoperative adjuvant treatments for precision medicine can be applied to patients with poor prognostic data.

Materials and Methods

Patients

The Local Ethics Committee of KTO Karatay University Faculty of Medicine approved this study under the decision number: 2021/010, number: E-41901325-050.99-2306. Patients who underwent an ^{18}F-FDG PET/CT scan before surgical resection with a diagnosis of ILA between August 2012 and September 2019 in our hospital were included in this study. Exclusion criteria were 1) neoadjuvant therapy before surgery, 2) tumor size of <10 mm (to eliminate partial volume effect on PET), (3) tumors with the SUV$_{max}$ lower than the determined MTV threshold of 2.5, 4) mucinous lung adenocarcinoma, and 5) inappropriate condition for ^{18}F-FDG PET/CT (fasting blood glucose of >150 mg/dL). The flowchart of patient selection is shown in Figure 1.

Clinicopathological data included age, sex, histopathological subtypes, tumor diameter, lymph node metastasis status, stage, and ^{18}F-FDG PET/CT parameters. The tumor diameter,
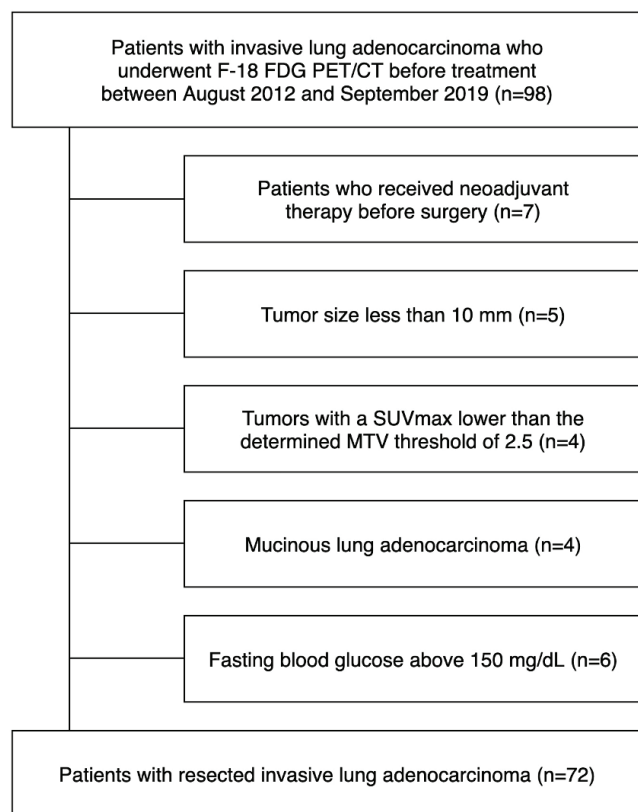
Figure 1. The flowchart of patient selection
^{18}F-FDG: [18]Fluorine-fluorodeoxyglucose, PET/CT: Positron emission tomography/computed tomography

nodal involvement, and metastasis (TNM) stage are based on the 8th edition of the American Joint Committee on Cancer TNM classification for lung cancer (17). The following five histopathological subtypes of ILA were determined according to the predominant pattern: LA, AA, PA, SA, and MA. Only two patients had MA patterns, thus they were merged under the SA-MA group, as both solid and micropapillary patterns are considered high-grade.

After the primary tumor resection, all patients underwent regular clinical follow-up, including physical examination and CT or scans every 3-6 months. In cases of abnormal findings on these follow-up examinations, additional imaging studies, including contrast-enhanced CT and ^{18}F-FDG PET/CT scans were performed to verify local, regional, or distant relapse. Therefore, PFS was defined as the time between the dates of pre-operative ^{18}F-FDG PET/CT scan and the date of relapse in patients with relapsed, whereas the time between the date of the ^{18}F-FDG PET/CT scan and the last visit to the hospital for ILA in patients with non-relapsed. The onset for OS was the date of the pre-operative ^{18}F-FDG PET/CT scan. Patient relatives were called by telephone. The telephone follow-up date for the

survivors and the date of death for the non-survivors were considered the OS endpoint.

Imaging

Patients fasted for 6-8 hours, and ^{18}F-FDG (3.7 MBq/kg) was intravenously injected when their fasting blood glucose was <150 mg/dL. Patients were rested for 60 min after the injection and underwent PET/CT (Biograph LSO-16 PET/CT scanner, Siemens Medical Solutions, Chicago, IL) scan using ^{18}F-FDG. The scan was done from the base of the skull to the upper part of the thigh. CT scan parameters were 120 kV, 140 mAs, and slice thickness of 5 mm. PET acquisition method was 3 min/bed. Images were generated using the reconstruction method with PET and CT. PET/CT fusion images were obtained and transferred to the workstation.

Image Analysis

An experienced nuclear medicine physician has visually and semi-quantitatively analyzed ^{18}F-FDG PET/CT images. A region of interest (ROI) was drawn around the tumor to calculate SUV_{max} and mean SUV (SUV_{mean}) values. A volume of interest with an SUV threshold of 2.5 was used to determine the MTV using the software program (TRUE D, Siemens Medical Solutions). TLG was obtained by multiplying the MTV by the SUV_{mean}.

Textural Analysis

The ^{18}F-FDG PET images were evaluated by LIFEx v6.30 software, a semi-automatic program for three-dimensional histogram-based textural analysis (18). Figure 2 shows the extraction of tumor HBTFs from ^{18}F-FDG PET images. The SUV_{max} threshold of 2.5 was used for tumor segmentation, and the reproducibility of extracted TFs using this value was better compared to other threshold values (19). The TFs obtained from the primary tumor consisted of HBTFs (skewness, kurtosis, energy-uniformity, and entropy). Second- and higher-level TFs were extracted from lesions larger than 64 voxels. However, these parameters were not evaluated as a significant amount of tumors (30/72) in the study population below this level.

Statistical Analysis

Study variables were analyzed using Statistical Package for the Social Sciences v26 (IBM Corporation, Armonk, NY, USA). The data were not homogeneously distributed. Therefore, the data were expressed as medians. The Mann-Whitney U test was used for comparisons between paired groups, whereas the Kruskal-Wallis test was for multiple group comparisons. Significance values have been adjusted by the Bonferroni correction for multiple tests.

A Cox regression model including parameters with p values of <0.05 in the univariate analysis was used to
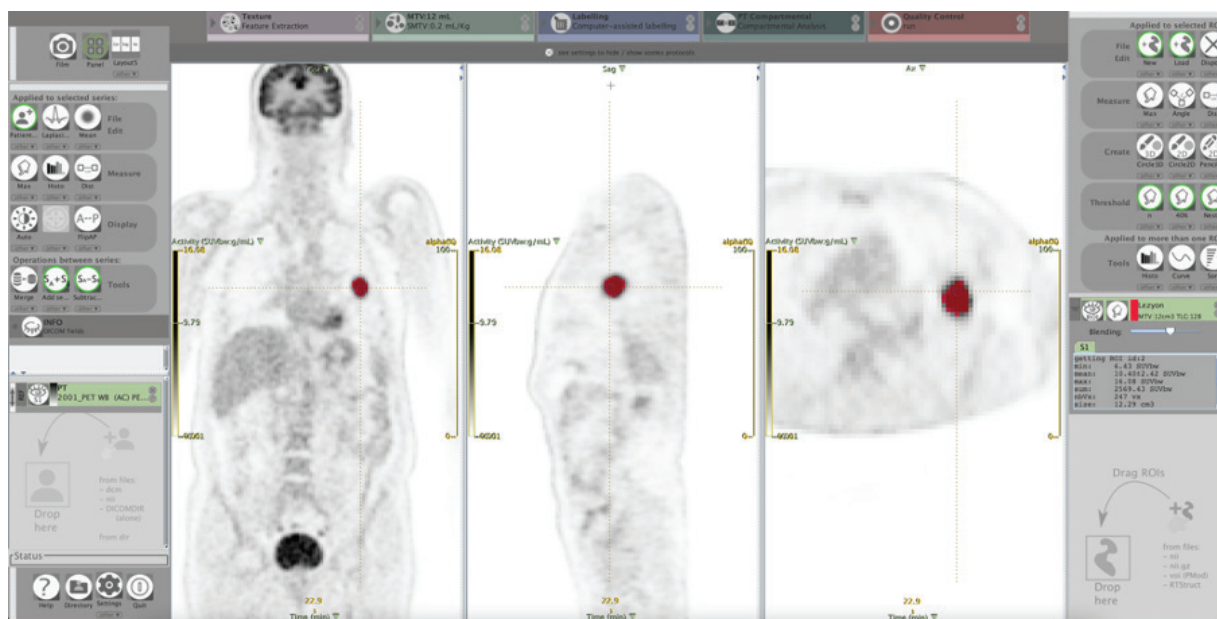
Figure 2. Demonstration of tumor HBTF extraction from ¹⁸F-FDG PET image
HBTF: Histogram-based textural feature, ¹⁸F-FDG: ¹⁸Fluorine-fluorodeoxyglucose, PET: Positron emission tomography

determine covariates for the multivariate analyses. Using these covariates, multivariate Cox regression models were constructed. Hazard ratios (HR) and 95% confidence interval (CI) were calculated. Differences were considered statistically significant at a p value of <0.05.

Results

This study included 72 patients with ILA with a mean age of 63.8±9.7 years, of whom 21 (29.2%) were females and 51 (70.8%) were males. All participants underwent clinically selected appropriate surgical treatment [wedge resection (9), lobectomy (56), and pneumonectomy (7)] in a median duration of 19 (13-32) days after ¹⁸F-FDG PET/CT scan. Of these patients, 35 (48.6%) received postoperative adjuvant treatments. The clinicopathological characteristics of patients are summarized in Table 1.

The histopathological subtypes were as follows: 43 (59.7%) AA, 15 (20.8%) SA, 7 (9.8%) LA, 5 (6.9%) PA, and 2 (2.8%) MA. The SUV$_{max}$, MTV, TLG, energy-uniformity, and entropy values significantly differed between the histopathological subtypes (p values: 0.003, 0.002, 0.003, 0.022, and 0.041, respectively). In post-hoc analyses, the median SUV$_{max}$ and entropy values of the SA-MA were significantly higher, whereas significantly lower in LA. The median MTV and TLG values were significantly higher in PA and lower in LA. A significant difference was found between the LA and SA-MA in MTV. Additionally, significant differences were found in TLG between the LA and PA, and between the LA and SA-MA.

The median energy-uniformity value was significantly higher in the LA and lower in the SA-MA. Table 2 demonstrates the comparison of ¹⁸F-FDG PET/CT parameters between the subtype groups. Figure 3 shows the representative ¹⁸F-FDG PET/CT images and hematoxylin-eosin-stained samples of two different histopathological ILA subtypes.

Tumor diameter was strongly correlated with MTV and TLG (r=0.742 and 0.709, respectively, both p=<0.001). SUV$_{max}$ and entropy had weak positive correlations with tumor diameter (r=0.305 and p=0.009; r=0.412 and p=<0.001, respectively). Skewness, kurtosis, and energy-uniformity had weak and negative correlation with tumor diameter (r=-0.383, -0.406, and -0.445; p=0.001, <0.001, and 0.003, respectively). Lymph node involvement was observed in 21 (29.2%) patients. Among all parameters, only skewness and kurtosis significantly differed between patients with or without lymph node involvement. In those with lymph node involvement, the median skewness and kurtosis values of the tumor were significantly lower than those without lymph node involvement (median skewness: 2.46 and 1.76, respectively, p=0.009; median kurtosis: 8.78 and 5.29, respectively, p=0.008). Significant differences were found between the stage groups in terms of MTV, TLG, skewness, and kurtosis parameters (p=0.001, 0.001, 0.022, and 0.025, respectively). Higher median MTV and TLG values and lower median skewness and kurtosis values were seen in higher-stage tumors. In post-hoc analyses, differences were observed for MTV and TLG between stages 1A and 2A (p=0.003 and 0.005, respectively),
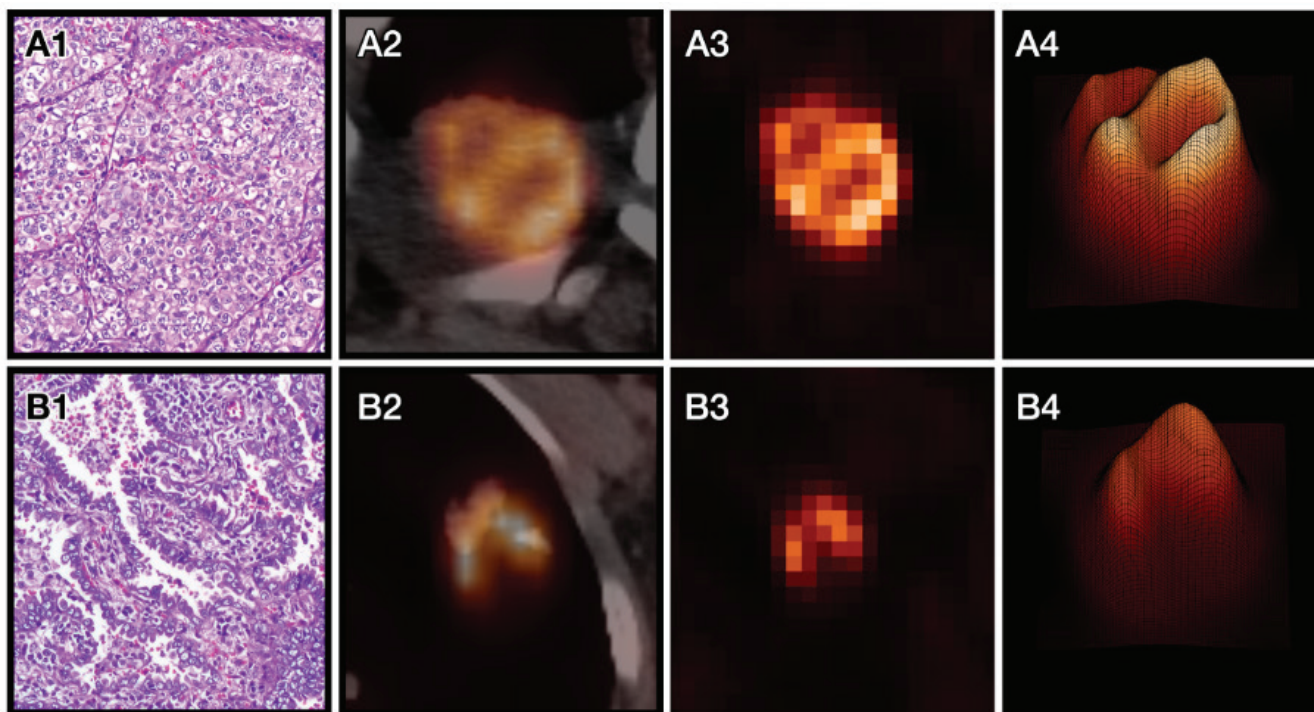
Figure 3. (A) Patient with invasive lung adenocarcinoma of the right upper lobe. Hematoxylin and eosin staining (H&E) (A1) demonstrates the histopathological subtype of lepidic adenocarcinoma (H&E × 100). Transaxial PET/CT image shows invasive lung adenocarcinoma of the right upper lobe with increased ^{18}F-FDG uptake (A2) and relatively lower intra-tumoral heterogeneity (A3 and A4). SUV_{max} of 8.42, the entropy of 1.1387, and energy-uniformity of 0.0848. (B) Patient with invasive lung adenocarcinoma of the left upper lobe. H&E staining (B1) demonstrates the histopathological subtype of solid adenocarcinoma (H&E × 100). Transaxial PET/CT image shows invasive lung adenocarcinoma of the left upper lobe with increased ^{18}F-FDG uptake (B2) and relatively higher intra-tumoral heterogeneity (B3 and B4). SUV_{max} of 47.70, the entropy of 1.7000, and energy-uniformity of 0.0200

SUV_{max}: Maximum standardized uptake value, ^{18}F-FDG: [18]Fluorine-fluorodeoxyglucose, PET/CT: Positron emission tomography/computed tomography

stages 1A and 2B (both p=0.001), and stages 1A and 3A (both p=0.002). Additionally, differences were observed for skewness and kurtosis between stages 1A and 3A (p=0.038 and 0.021, respectively).

The median values for follow-up time, PFS, and OS were 31.26, 16.07, and 20.87 months, respectively. During the follow-up time, 33 (45.8%) patients had a relapse and 20 (27.8%) patients died. The univariate Cox regression analyses showed that lymph node involvement was the only significant predictor factor for PFS (HR: 2.101, CI: 1.025-4.039, p=0.043) (Table 3). Univariate Cox regression analyses showed that high tumor diameter (≥3 cm), lymph node involvement, high stage (IIB-IIIA), high SUV_{max} (≥11.69), high MTV (≥9.02 cm³), high TLG (≥48.38 g), low skewness (≤2.18), low kurtosis (≤7.16), low energy-uniformity (≤0.08), and high entropy (≥1.24) were risk factors that affect the OS (Table 4). The multivariate Cox regression analysis revealed that high SUV_{max} (≥11.69) and advanced stage (IIB-IIIA) was negative independent predictors of OS (Table 5).

Discussion

This study investigated the relationship of ^{18}F-FDG PET/CT parameters, including HBTFs, between clinicopathological factors that affect TH and ILA prognosis. Significant differences were found between the conventional parameters of ^{18}F-FDG PET/CT (SUV_{max}, MTV, and TLG), as well as HBTFs such as entropy and energy-uniformity, and histopathological ILA subtypes. The group consisting of SA and MA had high glycolytic activity and entropy, whereas LA had low glycolytic activity and entropy. Additionally, SA-MA had the lowest energy-uniformity, whereas LA had the highest. Among the ^{18}F-FDG PET/CT parameters, only skewness and kurtosis were associated with lymph node involvement.

TH is an important factor in disease progression and treatment response (20,21). A study that involve patients with advanced lung adenocarcinoma with epidermal growth factor receptor mutation who received tyrosine kinase inhibitor therapy revealed a shorter survival in patients with primary tumors with high entropy values. Additionally, they

Table 1. Patients characteristics

	N	%
Age (years)		
<65	35	48.6
≥65	37	51.4
Sex		
Male	51	70.8
Female	21	29.2
Lymph node involvement		
Positive	21	29.2
Negative	51	70.8
Stage		
IA	30	41.6
IB	3	4.2
IIA	4	5.6
IIB	15	20.8
IIIA	20	27.8
Subtype		
Acinar	43	59,7
Solid	15	20.8
Lepidic	7	9,8
Papillary	5	6,9
Micropapillary	2	2,8
Operation type		
Wedge resection	9	12.5
Lobectomy	56	77.7
Pneumonectomy	7	9.8
Adjuvant therapy		
Yes	35	48.6
No	37	51.4

Table 2. Comparison of the median values of ^{18}F-FDG PET/CT parameters in histopathological subtypes of invasive lung adenocarcinoma groups

	AA	LA	PA	SA-MA	p value
SUV_{max}	12.07	6.82	10.68	14.89	0.003
MTV	9.11	1.00	63.27	10.08	0.002
TLG	48.82	4.08	275.17	56.87	0.003
Skewness	2.10	3.22	1.91	2.14	0.094
Kurtosis	7.97	12.78	5.06	6.14	0.081
Energy-uniformity	0.0714	0.1424	0.0776	0.0610	0.022
Entropy	1.1385	0.8865	1.1816	1.2539	0.041

Underline indicates statistical insignificance. ^{18}F-FDG: [18]Fluorine-fluorodeoxyglucose, PET/CT: Positron emission tomography/computed tomography, AA: Acinar adenocarcinoma, LA: Lepidic adenocarcinoma, PA: Papillary adenocarcinoma, SA-MA: Solid and micropapillary adenocarcinoma; SUV_{max}: Maximum standardized uptake value, MTV: metabolic tumor value, TLG: Total lesion glycolysis

Table 3. The univariate Cox regression analysis of progression-free survival in patients with invasive lung adenocarcinoma

Variables	HRs	95% confidence intervals	p value
Age (≤65)	0.897	(0.452-1.780)	0.757
Sex (male)	0.940	(0.454-1.944)	0.867
Lymph node involvement (yes)	2.101	(1.025-4.309)	0.043
Stage (IIB-IIIA)	1.920	(0.957-3.855)	0.067
Diameter (≥3 cm)	1.365	(0.658-2.832)	0.403
SUV_{max} (≥11.69)	1.246	(0.625-2.482)	0.532
MTV (≥9.02 cm³)	1.385	(0.695-2.760)	0.354
TLG (≥48.38 g)	1.104	(0.556-2.191)	0.778
Skewness (≤2.18)	1.267	(0.636-2.525)	0.501
Kurtosis (≤7.16)	1.229	(0.869-1.738)	0.243
Energy-uniformity (≤0.08)	1.486	(0.743-2.972)	0.262
Entropy (≥1.14)	1.763	(0.880-3.532)	0.110

HRs: Hazard ratios, SUV_{max}: Maximum standardized uptake value, MTV: Metabolic tumor value, TLG: Total lesion glycolysis

reported that entropy value is an independent predictor of treatment response and decreases after treatment (22). According to Hyun et al. (23) lower entropy was independently associated with longer survival in patients with pancreatic ductal adenocarcinoma. In their study on breast cancer, Aide et al. (13) reported that tumors with high entropy and low energy-uniformity have shorter event-free survival, but the log-rank tests reached almost statistical significance. The evidence is insufficient, but all these results suggest that precision medicine will improve with the use of TFs. Our study revealed entropy and energy-uniformity as predictors of OS, but they were not among the independent predictors for OS and PFS in multivariate Cox regression analysis. Higher SUV_{max} (≥11.69) and advanced stage (IIB-IIIA) was significantly associated with poorer OS in our study population.

Entropy and energy-uniformity quantitatively characterize the TH from various perspectives. Entropy refers to the randomness of voxel intensity distribution within the ROI. Entropy increases as the intensities of pixels are chaotically distributed. Energy-uniformity measures the number of repeated pairs. Thus, it reflects the distribution uniformity. This parameter is expected to increase as the number of repeated pixel pairs increases (21). Our findings suggest that SA-MA subtypes have high TH and higher metabolism, whereas LA is more homogeneous with a lower metabolism. Previous study that examine the relationship between the

Table 4. The univariate Cox regression analysis of overall survival in patients with invasive lung adenocarcinoma

Variables	Univariate Cox regression analysis		
	HRs	95% confidence intervals	p values
Age (≤65)	1.200	(0.495-2.909)	0.687
Sex (male)	0.406	(0.134-1.235)	0.112
Lymph node involvement (yes)	2.512	(1.043-6.053)	0.040
Stage (IIB-IIIA)	8.871	(2.050-38.398)	0.004
Diameter (≥3 cm)	3.778	(1.474-9.681)	0.006
SUV$_{max}$ (≥11.69)	4.329	(1.442-12.996)	0.009
MTV (≥9.02 cm³)	4.495	(1.490-13.563)	0.008
TLG (≥48.38 g)	3.488	(1.253-9.709)	0.017
Skewness (≤2.18)	2.918	(1.056-8.067)	0.039
Kurtosis (≤7.16)	1.761	(1.060-2.929)	0.029
Energy-uniformity (≤0.08)	3.144	(1.137-8.693)	0.027
Entropy (≥1.14)	3.027	(1.097-8.352)	0.032

HRs: Hazard ratios, SUV$_{max}$: Maximum standardized uptake value, MTV: Metabolic tumor value, TLG: Total lesion glycolysis

Table 5. Independent predictors of overall survival in patients with invasive lung adenocarcinoma

Variables	The multivariate Cox regression analysis		
	HRs	95% confidence intervals	p value
High stage (IIB-IIIA)	7.608	(1.756-32.973)	0.007
High SUV$_{max}$ (≥11.69)	3.580	(1.186-10.806)	0.024

SUV$_{max}$: Maximum standardized uptake value

histopathological subtypes of ILA and SUV$_{max}$ report that SA had higher SUV$_{max}$ than LA (24). The presence of the SA or MA subtype is a poor prognostic factor (25). According to these findings, the poor prognosis of the SA-MA group may be due to TH and higher metabolic activity.

Among all ^{18}F-FDG PET/CT parameters, only skewness and kurtosis were significantly different in lymph node involvement. These parameters show the distortion or disparity of the histogram that is relative to the normal distribution (18). A recent study described a machine learning-based TFs model as a reliable method for predicting axillary lymph node metastasis in invasive ductal breast cancer (26). Li et al. (27) found that skewness was the most ideal predictor for pelvic lymph node involvement in cervical squamous cell carcinoma. Our previous study revealed that a high-order TF showing the distribution of short homogeneous regions with low gray levels had

an independent association with axillary lymph node metastasis unlike other parameters of ^{18}F-FDG PET/CT in invasive ductal breast cancer (28).

However, texture analysis still has a reproducibility barrier to overcome before its clinical practice implementation (14,29). Additionally, TFs that are the most reliable indicator of TH for different tumor types are unclear. HBTFs are based on the analysis of the SUV histogram within the entire tumor. These parameters may have higher chances of clinical applicability in the future because of their simplicity and accessibility compared to more complex higher-order TFs. Most of the TFs are affected by tumor segmentation methods. The present study used the threshold of SUV of 2.5 for the tumor segmentation since the reproducibility of extracted TFs using this threshold was better than that of other thresholds (19). Various tumor segmentation techniques, such as manual or threshold-based methods, are used in the studies; however, no consensus is available on the most appropriate method for ^{18}F-FDG PET/CT textural analysis.

Study Limitations

Limitations of the study include the retrospective design, small sample size, and single-institution experience. Additionally, we cannot extrapolate the findings to patients with advanced stage ILA.

Conclusion

High stage and high SUV$_{max}$ were independent risk factors for OS in patients with ILA. The homogeneity of LA and the heterogeneity of SA-MA were quantified by HBTFs. Lymph node involvement was predicted by skewness and kurtosis. Therefore, HBTFs may improve the prognostic value of ^{18}F-FDG PET/CT by contributing to the quantification of TH. If confirmed by larger, prospective, and multi-center studies, extracted HBTFs from ^{18}F-FDG PET/CT could potentially become non-invasive prognostic imaging biomarkers to guide precision medicine.

Ethics

Committee Approval: The Local Ethics Committee of KTO Karatay University Faculty of Medicine approved this study under the decision number: 2021/010, number: E-41901325-050.99-2306.

Informed Consent: The informed consent form was obtained from the patients or their relatives who participated in the study.

Peer-review: Externally peer-reviewed.

Authorship Contributions

Surgical and Medical Practices: H.Ö., M.İ.E.K., Concept: H.Ö., M.İ.E.K., N.C., Design: H.Ö., N.C., Data Collection or Processing: H.Ö., N.C., Analysis or Interpretation: H.Ö., N.C., Literature Search: H.Ö., N.C., M.E., M.İ.E.K., Writing: H.Ö., N.C., M.E., M.İ.E.K.

References

1. Bray F, Ferlay J, Soerjomataram I, Siegel RL, Torre LA, Jemal A. Global cancer statistics 2018: GLOBOCAN estimates of incidence and mortality worldwide for 36 cancers in 185 countries. CA Cancer J Clin 2018;68:394-424. Erratum in: CA Cancer J Clin 2020;70:313.

2. Reck M, Popat S, Reinmuth N, De Ruysscher D, Kerr KM, Peters S; ESMO Guidelines Working Group. Metastatic non-small-cell lung cancer (NSCLC): ESMO Clinical Practice Guidelines for diagnosis, treatment and follow-up. Ann Oncol 2014;25 (Suppl 3):iii27-39.

3. Russell PA, Wainer Z, Wright GM, Daniels M, Conron M, Williams RA. Does lung adenocarcinoma subtype predict patient survival?: A clinicopathologic study based on the new International Association for the Study of Lung Cancer/American Thoracic Society/European Respiratory Society international multidisciplinary lung adenocarcinoma classification. J Thorac Oncol 2011;6:1496-1504.

4. Bedard PL, Hansen AR, Ratain MJ, Siu LL. Tumour heterogeneity in the clinic. Nature 2013;501:355-364.

5. Bashir U, Siddique MM, Mclean E, Goh V, Cook GJ. Imaging heterogeneity in lung cancer: techniques, applications, and challenges. AJR Am J Roentgenol 2016;207:534-543.

6. Chicklore S, Goh V, Siddique M, Roy A, Marsden PK, Cook GJ. Quantifying tumour heterogeneity in 18F-FDG PET/CT imaging by texture analysis. Eur J Nucl Med Mol Imaging 2013;40:133-140.

7. Zhang J, Ma G, Cheng J, Song S, Zhang Y, Shi LQ. Diagnostic classification of solitary pulmonary nodules using support vector machine model based on 2-[18F]fluoro-2-deoxy-D-glucose PET/computed tomography texture features. Nucl Med Commun 2020;41:560-566.

8. Nakajo M, Jinguji M, Aoki M, Tani A, Sato M, Yoshiura T. The clinical value of texture analysis of dual-time-point 18F-FDG-PET/CT imaging to differentiate between 18F-FDG-avid benign and malignant pulmonary lesions. Eur Radiol 2020;30:1759-1769.

9. Aydos U, Ünal ER, Özçelik M, Akdemir D, Ekinci Ö, Taştepe AI, Memiş L, Atay LÖ, Akdemir ÜÖ. Texture features of primary tumor on 18F-FDG PET images in non-small cell lung cancer: the relationship between imaging and histopathological parameters. Rev Esp Med Nucl Imagen Mol (Engl Ed) 2021;S2253-654X:30134-30137.

10. Önner H, Abdülrezzak Ü, Tutuş A. Could the skewness and kurtosis texture parameters of lesions obtained from pretreatment Ga-68 DOTA-TATE PET/CT images predict receptor radionuclide therapy response in patients with gastroenteropancreatic neuroendocrine tumors? Nucl Med Commun 2020;41:1034-1039.

11. Martin-Gonzalez P, de Mariscal EG, Martino ME, Gordaliza PM, Peligros I, Carreras JL, Calvo FA, Pascau J, Desco M, Muñoz-Barrutia A. Association of visual and quantitative heterogeneity of 18F-FDG PET images with treatment response in locally advanced rectal cancer: a feasibility study. PLoS One 2020;15:e0242597.

12. Kang J, Lee JH, Lee HS, Cho ES, Park EJ, Baik SH, Lee KY, Park C, Yeu Y, Clemenceau JR, Park S, Xu H, Hong C, Hwang TH. Radiomics features

13. of 18f-fluorodeoxyglucose positron-emission tomography as a novel prognostic signature in colorectal cancer. Cancers (Basel) 2021;13:392.

13. Aide N, Elie N, Blanc-Fournier C, Levy C, Salomon T, Lasnon C. Hormonal receptor immunochemistry heterogeneity and 18F-FDG metabolic heterogeneity: preliminary results of their relationship and prognostic value in luminal non-metastatic breast cancers. Front Oncol 2021;10:599050.

14. Nyflot MJ, Yang F, Byrd D, Bowen SR, Sandison GA, Kinahan PE. Quantitative radiomics: impact of stochastic effects on textural feature analysis implies the need for standards. J Med Imaging (Bellingham) 2015;2:041002.

15. Ercelep O, Alan O, Telli TA, Tuylu TB, Arıkan R, Demircan NC, Simsek ET, Babacan NA, Kaya S, Dane F, Bozkurtlar E, Ones T, Lacin T, Yumuk PF. Differences in PET/CT standardized uptake values involvement and survival compared to histologic subtypes of lung adenocarcinoma. Tumori 2021;107:231-237.

16. Chiu CH, Yeh YC, Lin KH, Wu YC, Lee YC, Chou TY, Tsai CM. Histological subtypes of lung adenocarcinoma have differential ^{18}F-fluorodeoxyglucose uptakes on the positron emission tomography/computed tomography scan. J Thorac Oncol 2011;6:1697-1703.

17. Goldstraw P, Chansky K, Crowley J, Rami-Porta R, Asamura H, Eberhardt WE, Nicholson AG, Groome P, Mitchell A, Bolejack V; International Association for the Study of Lung Cancer Staging and Prognostic Factors Committee, Advisory Boards, and Participating Institutions; International Association for the Study of Lung Cancer Staging and Prognostic Factors Committee Advisory Boards and Participating Institutions. The IASLC lung cancer staging project: proposals for revision of the TNM stage groupings in the forthcoming (eighth) edition of the TNM classification for lung cancer. J Thorac Oncol 2016;11:39-51.

18. Nioche C, Orlhac F, Boughdad S, Reuzé S, Goya-Outi J, Robert C, Pellot-Barakat C, Soussan M, Frouin F, Buvat I. LIFEx: a freeware for radiomic feature calculation in multimodality imaging to accelerate advances in the characterization of tumor heterogeneity. Cancer Res 2018;78:4786-4789.

19. Konert T, Everitt S, La Fontaine MD, van de Kamer JB, MacManus MP, Vogel WV, Callahan J, Sonke JJ. Robust, independent and relevant prognostic 18F-fluorodeoxyglucose positron emission tomography radiomics features in non-small cell lung cancer: are there any? PLoS One 2020;15:e0228793.

20. Gerlinger M, Rowan AJ, Horswell S, Math M, Larkin J, Endesfelder D, Gronroos E, Martinez P, Matthews N, Stewart A, Tarpey P, Varela I, Phillimore B, Begum S, McDonald NQ, Butler A, Jones D, Raine K, Latimer C, Santos CR, Nohadani M, Eklund AC, Spencer-Dene B, Clark G, Pickering L, Stamp G, Gore M, Szallasi Z, Downward J, Futreal PA, Swanton C. Intratumor heterogeneity and branched evolution revealed by multiregion sequencing. N Engl J Med 2012;366:883-892. Erratum in: N Engl J Med 2012;367:976.

21. Lemarignier C, Martineau A, Teixeira L, Vercellino L, Espié M, Merlet P, Groheux D. Correlation between tumour characteristics, SUV measurements, metabolic tumour volume, TLG and textural features assessed with 18F-FDG PET in a large cohort of oestrogen receptor-positive breast cancer patients. Eur J Nucl Med Mol Imaging 2017;44:1145-1154.

22. Chen YH, Wang TF, Chu SC, Lin CB, Wang LY, Lue KH, Liu SH, Chan SC. Incorporating radiomic feature of pretreatment 18F-FDG PET improves survival stratification in patients with EGFR-mutated lung adenocarcinoma. PLoS One 2020;15:e0244502.

23. Hyun SH, Kim HS, Choi SH, Choi DW, Lee JK, Lee KH, Park JO, Lee KH, Kim BT, Choi JY. Intratumoral heterogeneity of (18)F-FDG uptake predicts survival in patients with pancreatic ductal adenocarcinoma. Eur J Nucl Med Mol Imaging 2016;43:1461-1468.

24. Ventura L, Scarlattei M, Gnetti L, Silini EM, Rossi M, Tiseo M, Sverzellati N, Bocchialini G, Musini L, Balestra V, Ampollini L, Rusca M, Carbognani

P, Ruffini L. Prognostic value of [18F]FDG PET/CT parameters in surgically resected primary lung adenocarcinoma: a single-center experience. Tumori 2020;106:212-222.

25. Travis WD, Brambilla E, Nicholson AG, Yatabe Y, Austin JHM, Beasley MB, Chirieac LR, Dacic S, Duhig E, Flieder DB, Geisinger K, Hirsch FR, Ishikawa Y, Kerr KM, Noguchi M, Pelosi G, Powell CA, Tsao MS, Wistuba I; WHO Panel. The 2015 World Health Organization Classification of Lung Tumors: Impact of Genetic, Clinical and Radiologic Advances Since the 2004 Classification. J Thorac Oncol 2015;10:1243-1260.

26. Song BI. A machine learning-based radiomics model for the prediction of axillary lymph-node metastasis in breast cancer. Breast Cancer 2021;28:664-671.

27. Li K, Sun H, Lu Z, Xin J, Zhang L, Guo Y, Guo Q. Value of [18F]FDG PET radiomic features and VEGF expression in predicting pelvic lymphatic metastasis and their potential relationship in early-stage cervical squamous cell carcinoma. Eur J Radiol 2018;106:160-166.

28. Önner H, Coskun N, Erol M, Karanis MIE. Association of 18F-FDG PET/CT textural features with immunohistochemical characteristics in invasive ductal breast cancer. Rev Esp Med Nucl Imagen Mol (Engl Ed) 2021;S2253-654X:30201-30208.

29. Jha AK, Mithun S, Jaiswar V, Sherkhane UB, Purandare NC, Prabhash K, Rangarajan V, Dekker A, Wee L, Traverso A. Repeatability and reproducibility study of radiomic features on a phantom and human cohort. Nature 2021. doi.org/10.1038/s41598-021-81526-8.